Spalling Of High Strength Concrete Under Contact Explosive Charge

Duc Ngo The*, Thang Dam Trong, and Thuy Ngo Ngoc

Institute of Technical for Special Engineering, Le Quy Don Technical University, Hanoi, Vietnam

Corresponding author. E-mail: ducnt1988@lqdtu.edu.vn

Received: Aug. 27, 2024; Accepted: Mar. 19, 2025

Spalling is the phenomenon of concrete destruction under the impact of high-speed loads such as impact or explosion at the surface opposite to the load source. Spalling not only causes structural damage but also threats to humans and damages internal equipment by ejecting debris from the surface. Spalling in structures is induced by tensile waves, formed as incident waves propagate and are reflected the free surface (called reflected stress waves). In this study, experimental and simulation methods are applied to analyze the propagation and reflection process of stress waves,as well as the formation of spalling caused by reflected waves. These methods are also used to determine the spalling coefficient of high-strength concrete under contact charge. By changing the mass of the explosive charges and varying sizes of concrete slabs, the amount of explosives needed to induce spalling on each slab is determined. The spalling-resistant thickness is proportional to the relative mass of explosives. The results obtained are considered as a basis for determining the spalling-resistant thickness of protective structures faster and safer.

Keywords: Spalling damage, Blasting simulation and experimental, High-strength concrete, contact charge

© The Author('s). This is an open-access article distributed under the terms of the Creative Commons Attribution License (CC BY 4.0), which permits unrestricted use, distribution, and reproduction in any medium, provided the original author and source are cited.

http://dx.doi.org/10.6180/jase.202512_28(12).0017

1. Introduction

Spalling is a typical destructive phenomenon occurring as a structure is subjected to impulsive loads such as impacts or explosions. Furthermore, spalling can also occur due to other factors such as the expansion of steel reinforcement when corroded by oxidation or fire [1]. Within the scope of this study, only spalling caused by explosions is considered. As the explosive charge comes into contact with the structure, the part of the structure in contact with the explosion site will be destroyed forming a crater. On the opposite side, collapses may occur on the surface. This phenomenon is known as spalling by blasting. Depending on the mass of the explosive and the thickness of the structure, the spall funnel may be separate or connected to the crater with the explosive charge causing a structural breach.

Spalling may not necessarily lead to complete destruction or collapse of the structure; however, fragments ejected from the spall funnel may cause injury to people and equipment inside. Therefore, a study on the causes and destruction mechanisms of spalling phenomena is undertaken.

From the aspect of energy destruction, some authors believe that as the kinetic energy density of elements at the surface of the medium exceeds the specific destructive energy value, spalling will occur [2]. On this aspect, the authors have derived formulas to calculate the mass of explosives necessary to destroy the structure in proportion to the cube of the structure's thickness. However, this aspect does not account for the influence of the free surface. Moreover, in reality, some elements closer to the explosive take more energy but are not destroyed.

From the aspect of energy destruction, some authors believe that as the kinetic energy density of elements at the surface of the medium exceeds the specific destructive energy value, spalling will occur. On this aspect, the authors have derived formulas to calculate the mass of explosives necessary to destroy the structure in proportion to the cube

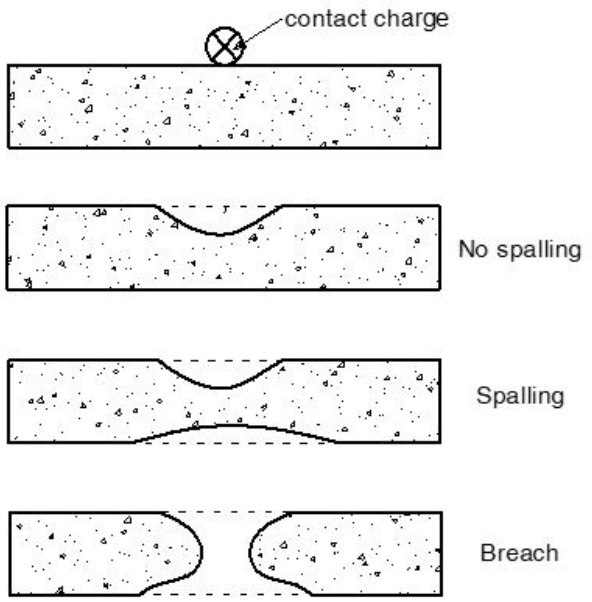

Fig. 1. Levels of damage on concrete slabs caused by contact explosions.

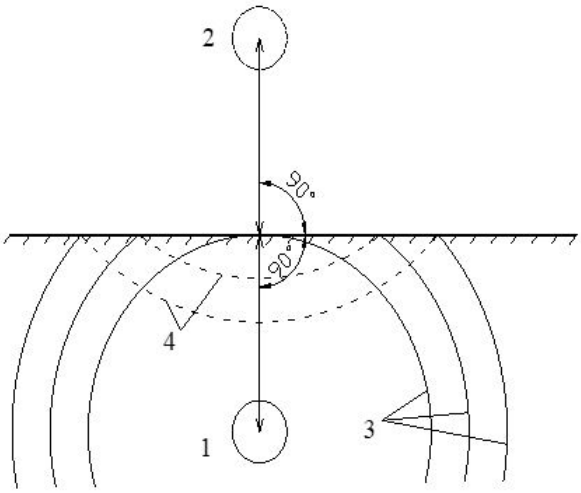

Fig. 2. Virtual explosion diagram explaining the formation of reflected waves. (1-Actual charge; 2-Virtual charge; 3-Incident waves; 4-Reflected stress waves.)

of the structure's thickness. However, this aspect does not account for the influence of the free surface. Moreover, in reality, some elements closer to the explosive take more energy but are not destroyed.

To explain the phenomenon of spalling, experts consider that blasting stress waves are the main cause of destruction. As stress waves propagate through environments with different acoustical properties or different cross-sectional areas, they undergo reflection and refraction. Depending on the acoustical properties of the medium, the intensity of stress waves may either increase or decrease [3].

After detonating the explosive charge, the pressure of the explosive products acts on the surface of the structure in contact with the explosive, causing stress waves to propagate within the structure. As the stress wave reaches the free surface, it is reflected, generating a reflected wave. The reflected wave tends to pull structural elements away from the surface. For brittle materials, the tensile strength of the material is often much smaller than the compressive strength ($\sigma t \ll \sigma c$), so the elements at the surface of the structure are destroyed and ejected [4–7].

Some authors consider that these tensile waves are generated by a virtual charge, equivalent and symmetrical to the actual charge through the free surface (Fig. 2). These tensile waves tend to pull medium particles toward the center of the virtual charge [7, 8].

The trend of using high-strength materials in protective structures is becoming increasingly common. High-strength concrete (HSC) and ultra-high-performance concrete (UHPC) are widely used in various constructions. Many authors have studied the behavior of high-strength and ultra-high-performance concretes under blast loading [9].

Through experimental studies on the collapse of structures subjected to explosive actions, McVay constructed graphs to determine the relationship between explosive mass, distance, and the thickness of the structure experiencing spalling phenomena [5].

Jun Li et al. conducted experimental studies on the distribution of particle size components after destruction due to the spalling phenomenon of ordinary concrete and ultra-high-performance concrete [9]. Lucionni et al. investigated the influence of steel fibers in high-strength concrete under static loads and explosions [10]. The trend of numerical simulations of UHPC and HSC behavior under blast impact through brittle material models such as the HJC model or the RHT model has also been pursued by many authors [11–13].

Fabricating structures using high-strength concrete materials is easier than using ultra-high-performance concrete, especially in the absence of modern construction equipment, in areas with complex terrain where deploying concrete quality control machinery is challenging, such as mountainous regions, islands, etc. Therefore, the study on spalling phenomena concerning these materials becomes essential.

When a structure is subjected to the blast effects of a

close-contact explosion, the immense pressure of the explosive products will act immediately on the elements adjacent to the explosion that causes destruction to these elements. At the same time, stress waves are generated and propagate within the structure.

When propagating outward, the intensity of the stress wave decreases and does not cause destruction to the material. However, when it encounters a free surface, the reflected stress waves are formed and tend to pull particles away from the surface. For convenience in the calculation, some authors assume that the reflected stress waves are generated from a virtual charge symmetrically equivalent to the actual charge through the free surface and tend to pull medium elements towards the center of the virtual charge [4].

Zhang proposed a contour method to describe and determine the intensity of stress wave propagation in materials. Additionally, the author also provided formulas to determine the conditions for spalling and the number of material layers separated when stress waves propagate to and reflect at the free surface [6]:

$$n = \frac{\sigma_{cm}}{\sigma_{td}} \quad \delta = \frac{1}{2n}\lambda \tag{1}$$

where n is the time of spalling, σ_{cm} is the amplitude of the compressive wave, σ_{td} is the dynamic tensile strength of the rock, δ is the thickness of each spalling, and λ is the length of the original compressive wave from the blast hole.

However, determining these parameters in practice is quite complicated. Based on the extent of the destruction, the blast effect range is divided into compression zones (crushing), fracture zones (cracking), and vibration zones. Based on analogous theory, almost authors affirm that the extent of these zones is proportional to cube root of explosive mass ($\sqrt[3]{C}$). Therefore, Xadopski proposed the following formula to determine these zones [14]:

$$\left.\begin{aligned} R_c &= m \cdot K_c \sqrt[3]{K_T \cdot C} \\ R_f &= m \cdot K_f \sqrt[3]{K_T \cdot C} \\ R_v &= m \cdot K_v \sqrt[3]{K_T \cdot C} \end{aligned}\right\} \tag{2}$$

where R_c, R_f, R_v are the radius of blast effect zones presented above, respectively, in meters; m is the confinement factor, depending on the arrangement conditions of the explosive charge, for contact detonation conditions $m = 1$; K_c, K_f, K_v are coefficients depending on the properties of the environment concerning the crushing, fracture, and vibration zones determined experimentally; K_T is the adjustment coefficient for the explosive charge according to the standard TNT explosive.

On this basis, one has the equation to determine the thickness of the structure to avoid destruction by spalling [14]:

$$R_S = mK_s \sqrt[3]{K_T C} \tag{3}$$

The formula above is widely used because it is simple and suitable for reality conditions. Once the coefficients K_c, K_f, K_v and K_s determined, one can quickly and easily determine various levels of destruction for structures subjected to explosions. Simultaneously, the thickness of protective structures against spalling is determined more quickly.

2. Materials and methods

2.1. Experimental

Based on Eq. (3), it is observed that the minimum spalling-resistant thickness of a concrete slab (R_s) is linearly proportional to the relative mass of the explosive charge ($\sqrt[3]{C}$). To determine the spalling coefficient for concrete, it is necessary to identify at least two points in the relationship between slab thickness and the relative mass of the explosive. Accordingly, experiments were conducted on two types of slabs with different dimensions and varying explosive charges to determine the critical explosive mass that causes spalling.

Concrete samples are made with two sizes (500x500x100)mm, (1000x1000x200)mm; surrounded by steel belt and installed crane hooks to facilitate erection. During manufacturing concrete panels, test samples are collected to test the concrete strength.

The high-strength concrete used in this study was mixed according to the mix proportions presented in Table 1. The compressive strength of the concrete was determined through compression tests conducted at different curing ages in the Materials Laboratory of Le Quy Don Technical University. The compressive strength value of the concrete at 28 days is presented in Table 1.

Table 1. Mix proportions for high-strength concrete.

MATERIAL	MASS
Cement (kg)	444
Sand (kg)	725
Gravel (kg)	1052
Water (kg)	163
Silicafume (kg)	44.4
Sikament NN (kg)	7.1

Based on the experimental results of concrete strength, to ensure structural safety under explosive loading, the value of concrete compressive strength fc =62.1 MPa was used for calculation.

Table 2. Compressive strength test results.

N^0	Compressive strength (N/mm ^{2})				
	R1	R3	R7	R14	R28
1	18.3	40.6	53.4	58.5	68.7
2	20	41.8	53.6	59.1	66.3
3	22.8	42.3	52.5	58.7	62.1

After the concrete slabs were fabricated and sufficient curing time was allowed for the concrete to reach the designed strength, the test specimens were placed on a support frame to create a free surface underneath (as illustrated in Fig. 3). The explosive charge was placed directly on the surface of the concrete slab at the midpoint between the two supports.

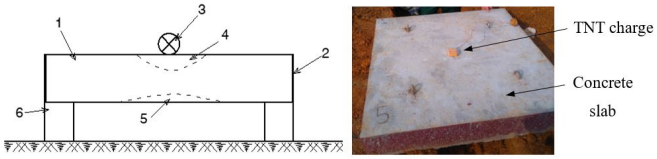

Fig. 3. Experimental layout.

where: 1. Concrete slab; 2. Steel belt covering concrete slabs; 3. Explosive amount; 4. Direct destruction zone; 5. Spalling zone; 6. Bracket.

Explosions are conducted on the surface of the panel using explosive charges of TNT with different masses to determine the amount of explosive that initiates the spalling.

2.2. Simulation

In addition to experimental methods, spalling studies of concrete can also be conducted through simulations. This method can be applied to various slab sizes and significantly reduces research costs.. In the present work, the ABAQUS/CAE software is used to simulate the effects of contact explosions on high-strength concrete structures. The concrete slab sizes used in the simulation study are 10 cm, 20 cm, and 30 cm, respectively.

2.2.1. *Concrete model*

The Homquit Johnson-Cook (HJC) model is used to model HSC material. The HJC material model is characterized by three equations: the stress-strain rate relationship equation, the damage equation through cumulative strain, and the static compression state equation [15–17].

The parameters of HSC with compressive strength according to the HJC model are calculated based on the research conducted by Ren et al. [18].

2.2.2. *Explosive model*

To model the pressure generated by TNT explosives, the John Wilke Lee's equation of state (JWL EoS) is used [19]:

$$p = A_1\left(1-\frac{\omega}{R_1V}\right)e^{-R_1V} + B_1\left(1-\frac{\omega}{R_2V}\right)e^{-R_2V} + \frac{\omega E_0}{V} \quad (4)$$

where V is the relative volume of the explosion products; A_1, B_1, R_1, R_2, and ω are characteristic parameters of the explosive charge obtained from experiments on the expansion of explosion products under controlled conditions [20]. These parameter values obtained from Bibiana Luccioni research [21].

3. Results and discussions

3.1. Experimental results

Fig. 4a corresponds to the case where the mass of explosives is just sufficient to induce spalling. And when increasing the mass of explosives, the level of destruction due to spalling also increases until the concrete slab is breached (Fig. 4b). The mass of explosives causing the spalling with the concrete slabs is presented in Table 3.

Table 3. The mass of explosive charges causing spalling on the HSC concrete panel.

Charge mass C (g)	Thickness of panel (Rs) (cm)
Dimension of concrete structure 1: (500x500x100)mm	
31,2	10
20,0	10
24,0	10
27,2	10
27,0	10
Dimension of concrete structure 2: (1000x1000x200)mm	
96,4	20
149,0	20
124,8	20

3.2. Simulation results

Forty-four cases of contact explosion simulations were conducted with 3 different panel thicknesses, 10cm, 20cm, and 30cm, respectively. The results are summarized in Figs. 5 to 7 and Table 4.

The simulation results of the concrete panel destruction with varying explosive charges are compiled in Table 4.

The process of stress wave propagation after detonating the explosive charge is illustrated in Fig. 7. When the stress wave reaches the free surface, it will be reflected at the free surface. As a result, the compressive stress waves will convert into tensile stress waves and propagate backward.

a

b

Fig. 4. Destruction caused by spalling on the back side of the concrete panel.

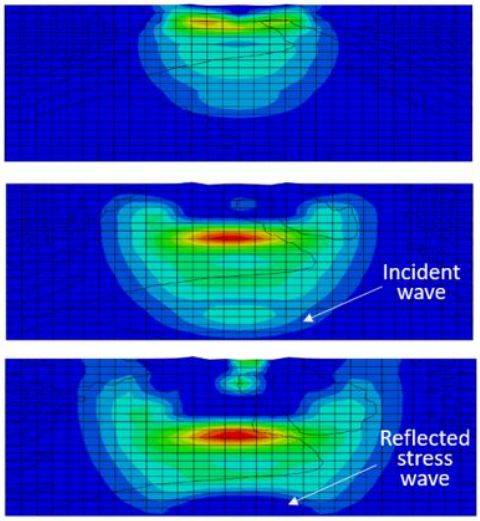

Fig. 5. The propagation and reflection of stress wave propagation in the concrete panel.

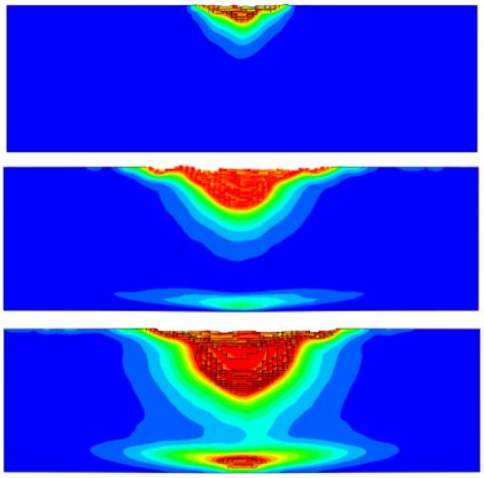

Fig. 6. The development of damage and the appearance of spalling in the concrete panel.

Fig. 6 describes the formation and development of destruction within the concrete panel. Similarly to the propagation process of stress waves, the development of damaged zones in the concrete slab also begins from the point of contact with the explosive charge, forming a crater. Spalling occurs after the stress waves are reflected at the free surface. If the tensile stress wave intensity exceeds the tensile strength of the concrete for a long enough time, it will cause spalling on the back surface.

From Fig. 7 it can be clearly seen that initially the concrete element near the free surface receives pressure from the incident compressive waves. This compressive stress forms compressive strains. But when the stress wave is reflected at the free surface, the compressive waves transform into tensile waves, immediately the compressive strains are also converted into tensile strains. Although the tensile stress reaches the tensile strength limit of concrete, failure does not occur immediately. Instead, the tensile stress must be sustained for a sufficient duration to allow tensile strain to accumulate until it reaches the failure threshold, at which point spalling occurs.

The results presented in Table 4 indicate that for a concrete slab with a thickness of 10 cm , when the explosive charge mass (m_c) is less than 18.16 g (explosive charge radius $r_c < 13.8$ mm), no spalling occurs. However, when $m_c \geq 18.16$ g, a spalling damaged zone appears, and even when $m_c \geq 28.3$ g, this concrete slab is breached.

Similarly, for concrete slabs with thicknesses of 20 cm and 30 cm , the explosive charge masses required to initiate spalling are 84.09 g and 400.59 g , respectively.

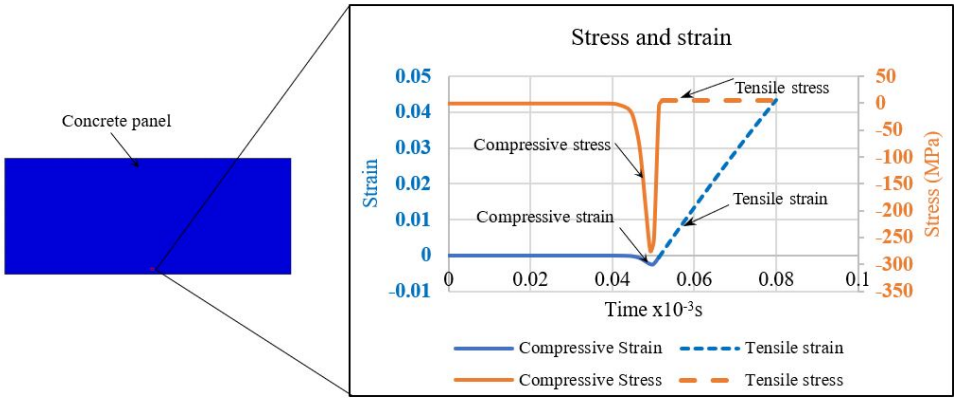

Fig. 7. Stress and strain of the spalling element follow the propagation direction of stress wave.

Table 4. Simulation results of the concrete panel destruction under the impact of the contact explosive charge.

Thickness of panel (m)	Charge mass (g)	**Radius of charge** (mm)	**The diameter of crater (m)**	**The deep of crater (m)**	**Description**
0.1	15.18	13	0.121	0.035	no spalling
	17.39	13.6	0.12205	0.0374	no spalling
	18.16	13.8	0.12412	0.035	spalling
	18.97	14	0.12463	0.0357	spalling
	28.31	16	0.138	-	breach
	33.96	17	0.145	-	breach
	36.41	17.4	0.15	-	breach
	55.29	20	0.1985	-	breach
0.2	40.31	18	0.155	0.0615	no spalling
	47.41	19	0.166	0.0805	no spalling
	55.29	20	0.1688	0.0807	no spalling
	64.01	21	0.175	0.0811	no spalling
	73.59	22	0.18975	0.0844	no spalling
	78.73	22.5	0.19495	0.0872	no spalling
	81.92	22.8	0.19585	0.0915	no spalling
	84.09	23	0.187	0.0965	spalling
	107.99	25	0.23495	0.1113	spalling
	151.72	28	0.28915	0.1173	spalling
	226.48	32	0.324	-	breach
0.3	226.48	32	0.304	0.0937	no spalling
	379.25	38	0.34475	0.1134	no spalling
	394.42	38.5	0.3835	0.1099	no spalling
	400.59	38.7	0.3691	0.1149	spalling
	409.98	39	0.37375	0.128	spalling
	442.34	40	0.3996	0.133	spalling
	476.35	41	0.394	0.139	spalling
	512.06	42	0.4075	0.141	spalling
	549.51	43	0.404	0.141	spalling
	629.81	45	0.4085	0.141	spalling
	672.74	46	0.413	0.141	spalling
	717.57	47	0.4585	0.141	spalling
	863.94	50	0.485	0.141	spalling

Compaprison of simulation and experimental result

The experimental and simulation data are presented in Tables 3 and 4, depicted by points in Fig. 8. The least squares method is used to obtain a graph illustrating the relationship between the thickness of the minimum spalling-resistant panel (Rs) and the relative explosive charge mass ($\sqrt[3]{C}$) according to the Eq. (2). From the graph, it can be observed that the minimum spalling-resistant thickness has a linear relationship with the relative mass of the explosive charge.

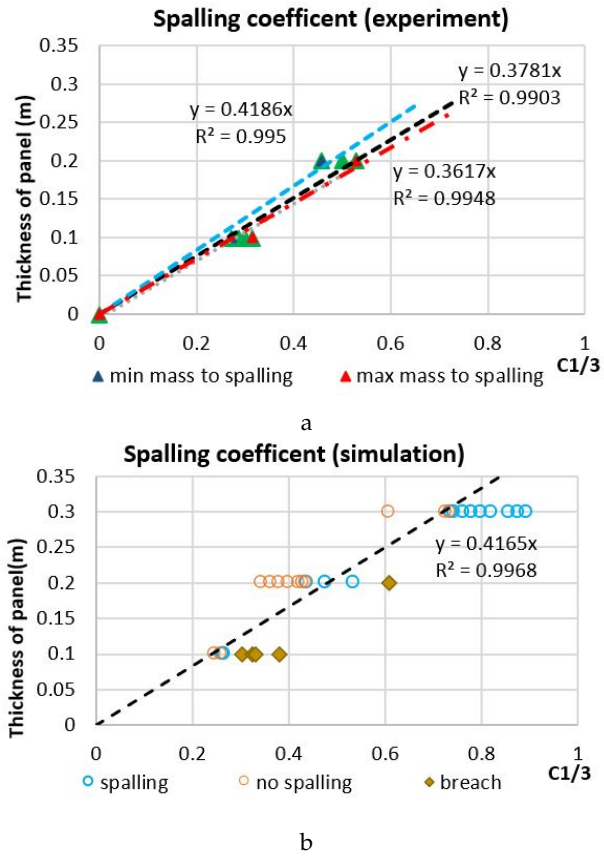

Fig. 8. Results of the spalling coefficient values based on the analysis of experimental and simulation data.

The graph in Fig. 8a represents the results obtained from experiments:

$$R_s = (0.4186 \div 0.3617)\sqrt[3]{C} \quad (5)$$

The results obtained from the simulation are shown in Fig. 8b:

$$R_s = 0.4165\sqrt[3]{C} \quad (6)$$

Based on the formulas presented, the spalling coefficient of high-strength concrete, determined through experimental methods, ranges from 0.3617 to 0.4186 , with an average value of 0.3781 . To apply the spalling coefficient in the design of protective structures subjected to direct surface explosions, a value of spalling coefficient $K_s = 0.4186$ is recommended to ensure the highest level of safety for personnel and internal equipment.

When using simulation methods, the spalling coefficient is found to be 0.4165 . This value is approximately equal to the experimentally obtained and previously recommended value. This finding indicates that the simulation model used in this study has high reliability and can be applied to analyze cases involving direct explosive loading with larger explosive masses and structural dimensions.

4. Conclusions

This study investigated the spalling phenomenon in high-strength concrete (HSC) structures subjected to close-contact explosions. Through both experimental and simulation approaches, the mechanisms leading to spalling were analyzed, and the relationship between the explosive charge and structural thickness was determined.

Experimental results confirmed that spalling occurs when the reflected tensile stress wave exceeds the dynamic tensile strength of the concrete. The experimental data demonstrated that the critical explosive mass required for spalling increases with structural thickness, consistent with theoretical predictions. Moreover, the simulation results using the Holmquist-Johnson-Cook (HJC) material model and the Jones-Wilkins-Lee (JWL) equation of state provided insights into stress wave propagation and material failure mechanisms. The simulated data aligned well with the experimental findings, validating the numerical approach as a cost-effective alternative for studying blast effects on HSC.

A key outcome of this study is the determination of the spalling coefficient for HSC. The experimental analysis yielded a coefficient ranging from 0.3617 to 0.4186, with a recommended design value of 0.4186 for protective structures to ensure maximum safety. The simulation-derived coefficient of 0.4165 further supports this recommendation, demonstrating the reliability of numerical modeling in predicting spalling behavior.

The findings of this study serve as a valuable reference for the design of blast-resistant structures, particularly in challenging environments that demand high-strength materials. Future research could focus on investigating spalling phenomena under various conditions, such as structures embedded in soil or submerged underwater. Additionally, exploring reinforcement strategies to enhance the spall resistance of concrete structures is highly relevant. Such measures not only mitigate damage to personnel and equipment within the protected area but also improve the structural integrity and load-bearing capacity of blast-resistant designs.

Acknowledgment

This study was supported by the Material Laboratory at Le Quy Don Technical University, Hanoi, Vietnam. The authors are very grateful to the experts for their constructive comments.

References

[1] R. Aldarf, M. Al-Allaf, A. Salem, H. Meree, F. Mubark, and B. Akkari, (2024) *"Fire Performance of Reinforced Concrete Slabs: Direct Flame Effects"* **Jordan Journal of Civil Engineering *18***(1): DOI: 10.14525/JJCE.v18i1.08.

[2] N. Q. Trung and V. T. Tung. *Explosive*. Ha Noi: Le Quy Don Technical University, 2005.

[3] F. Fraige and M. Es-Saheb, (2022) *"Analysis of Elastic Stress Wave Propagation in Stepped Bars, Transmission, Reflection, and Interaction: Experimental Investigation"* **Jordan Journal of Mechanical and Industrial Engineering *16***: 261–274. DOI: 10.14525/JJCE.v18i1.08.

[4] D. T. Thang, B. X. Nam, and T. Q. Hieu. *Blasting in mining and construction*. Ha Noi: Publishing House of Natural Science and Technology, 2015.

[5] M. K. McVay. *Spall damage of concrete structures*. US Army Engineer Waterways Experiment Station, 1988.

[6] Z.-X. Zhang. *Rock fracture and blasting: theory and applications*. Butterworth-Heinemann, 2016.

[7] E. O. Mindeli, N. F. Kusov, A. A. Sornayev, and G. I. Martsinkevich. *Investigation of Stress Waves During Explosions in Rocks*. 1978. URL: https://cir.nii.ac.jp/crid/1130282270471886720.

[8] H. S. Giao, D. T. Thang, L. V. Quyen, and H. T. Trung. *Chemical Explosions - Theory and Practice*. Ha Noi: Science and Technology Publishing House, 2010.

[9] J. Li, C. Wu, H. Hao, Z. Wang, and Y. Su, (2016) *"Experimental investigation of ultra-high performance concrete slabs under contact explosions"* **International Journal of Impact Engineering *93***: 62–75. DOI: 10.1016/j.ijimpeng.2016.02.007.

[10] B. Luccioni, F. Isla, R. Codina, D. Ambrosini, R. Zerbino, G. Giaccio, and M. C. Torrijos, (2017) *"Effect of steel fibers on static and blast response of high strength concrete"* **International Journal of Impact Engineering *107***: 23–37. DOI: 10.1016/j.ijimpeng.2017.04.027.

[11] Z. Wang, Y. Huang, and F. Xiong, (2019) *"Three-dimensional Numerical Analysis of Blast-induced Damage Characteristics of the Intact and Jointed Rockmass"* **Computers, Materials & Continua *58***: 1189–1206. DOI: 10.32604/cmc.2019.04972.

[12] Z. Wang, H. Wang, J. Wang, and N. Tian, (2021) *"Finite element analyses of constitutive models performance in the simulation of blast-induced rock cracks"* **Computers and Geotechnics *135***: 104172. DOI: 10.1016/j.compgeo.2021.104172.

[13] M. Žmindák, Z. Pelagić, P. Pastorek, M. Močilan, and M. Vybošťok, (2016) *"Finite element modelling of high velocity impact on plate structures"* **Procedia Engineering *136***: 162–168. DOI: 10.1016/j.proeng.2016.01.191.

[14] N. T. Ta, V. D. Loi, and D. V. Dich. *Fortifications - 1*. Ha Noi: Le Quy Don Technical University, 2008.

[15] D. T. Thang, N. T. Duc, and N. N. Thuy. *Research on the attenuation of blasting stress wave while propagation in limestone*. 2023. URL: https://tapchixaydung.vn/nghien-cuu-su-suy-giam-song-ung-suat-no-khi-lan-truyen-trong-moi-truong-da-voi-20201224000020657.html.

[16] T. J. Holmquist, G. R. Johnson, and W. H. Cook. *A Computational Constitutive Model for Concrete Subjected to Large Strains, High Strain Rates and High Pressures*. 1993. URL: https://www.tib.eu/de/suchen/id/BLCP%3ACN008959584.

[17] C. Oucif and L. M. Mauludin, (2019) *"Numerical modeling of high velocity impact applied to reinforced concrete panel"* **Underground Space *4***(1): 1–9. DOI: 10.1016/j.undsp.2018.04.007.

[18] G.-M. Ren, H. Wu, Q. Fang, and X.-Z. Kong, (2017) *"Parameters of Holmquist–Johnson–Cook model for high-strength concrete-like materials under projectile impact"* **International Journal of Protective Structures *8***(3): 352–367. DOI: 10.1177/2041419617721552.

[19] A. Alia and M. Souli, (2006) *"High explosive simulation using multi-material formulations"* **Applied Thermal Engineering *26***(10): 1032–1042. DOI: 10.1016/j.applthermaleng.2005.10.018.

[20] R. Castedo, J. Sanchidrián, L. López, P. Segarra, and A. Santos, (2015) *"Determination of the JWL Constants for ANFO and Emulsion Explosives from Cylinder Test Data"* **Central European Journal of Energetic Materials *12***: 177–194.

[21] B. Luccioni, D. Ambrosini, G. Nurick, and I. Snyman, (2009) *"Craters produced by underground explosions"* **Computers & Structures *87***(21): 1366–1373. DOI: 10.1016/j.compstruc.2009.06.002.